

## Molecular dynamics simulation of liquid water at 523 K

This article has been downloaded from IOPscience. Please scroll down to see the full text article.

1994 J. Phys.: Condens. Matter 6 2283

(<http://iopscience.iop.org/0953-8984/6/12/002>)

View [the table of contents for this issue](#), or go to the [journal homepage](#) for more

Download details:

IP Address: 171.66.16.147

The article was downloaded on 12/05/2010 at 17:57

Please note that [terms and conditions apply](#).

## Molecular dynamics simulation of liquid water at 523 K

J A Padró†§, J Martí†‡ and E Guàrdia†

† Departament de Física Fonamental, Universitat de Barcelona, Diagonal 647, 08028 Barcelona, Spain

‡ Departament de Física i Enginyeria Nuclear, Universitat Politècnica de Catalunya, Sor Eulàlia d'Anzizu B4-B5, 08034 Barcelona, Spain

Received 8 June 1993, in final form 22 November 1993

**Abstract.** Liquid water at 523 K is simulated assuming a flexible single-point-charged (SPC) potential. Both structural and dynamical properties at this temperature are compared with those at 298 K. The resulting structure and self-diffusion coefficient are in satisfactory agreement with the experimental data. The frequency peaks in the spectral densities are also in accord with the experimental infrared spectra. It has been shown that the changes of the properties are related to the degree of hydrogen bonding. When the temperature increases from 298 K to 523 K many hydrogen bonds vanish (40%) and the number of oxygen atoms with two or more direct hydrogen bonds is dramatically reduced (70%). Thus, the tridimensional hydrogen bond network, which is typical of liquid water at room and lower temperatures, is substantially destroyed at 523 K.

### 1. Introduction

Liquid water at room and lower temperatures has been extensively studied by both experimental and computer simulation methods. However, little attention has been paid to the study of the microscopic properties of water at high temperatures. Recent neutron diffraction measurements on heavy water at 523 K [1] have shown a marked weakening of the tetrahedral ordering which characterizes the structure of liquid water at room and lower temperatures. It has also been shown in [1] that the total intermolecular structure obtained by molecular dynamics (MD) simulation using a rigid polarizable water model which includes many-body contributions (NEMO) [2] is in agreement with the neutron diffraction data. However, MD simulations with the NEMO (non-empirical molecular orbital) potential are very expensive (the computer time is roughly six or seven times longer than that using a rigid non-polarizable potential [2]). It should be pointed out that it is highly advantageous to have available simple but realistic potentials for water, especially for applications of MD to the study of complex systems such as macromolecules or chemical processes in aqueous solutions.

In this work we use a flexible version of the single-point-charged (SPC) potential [3]. This potential is a three-centre model which is able to reproduce the main features of the microscopic behaviour of water at room temperature [2–5] with less computational cost than using polarizable models like NEMO. The SPC potential is one of the most widely used in recent MD studies of liquid water and aqueous systems. One of the advantages of the SPC model which is particularly relevant for this work is that intramolecular degrees of freedom can easily be included [4–6]. Thus, the infrared (IR) spectra corresponding to the molecular

§ To whom correspondence should be addressed.

vibrations may be investigated. Moreover, it should be noted that the properties of water at room temperature calculated by MD are not significantly improved when the SPC potential is replaced by NEMO and the dynamic properties are better reproduced with the SPC model [2].

The ability of the SPC potential to reproduce the properties of liquid water at high temperatures is checked in this paper. Both structural and dynamic properties (self-diffusion coefficient, IR spectra) at 523 K have been calculated and compared with available experimental data. MD simulations of water at 298 K have also been carried out. Since the changes of properties when  $T$  increases may be associated with a substantial reduction of hydrogen bonding, we have also analysed the number and characteristics of hydrogen bonds (HBs) at both temperatures.

## 2. Molecular dynamics simulations

We carried out MD simulations of 216 water molecules at  $T = 523$  K and  $\rho = 0.75$  g cm<sup>-3</sup> assuming a flexible SPC potential [5]. The OH and HH vibrations were modelled by a Morse and a harmonic potential, respectively. This intramolecular potential has the same form as that originally proposed by Toukan and Rahman [6] but the parameters were slightly modified for a better reproduction of the IR spectra of water at room temperature [5]. The Ewald method was used for the computation of the Coulombian interactions. The equations of motion were integrated by a leap-frog Verlet integration algorithm with coupling to a thermal bath. Because of the high frequency of the intramolecular vibrations a small integration time-step was used (0.5 fs). The same potential model was used in the MD simulations at  $T = 298$  K and  $\rho = 1$  g cm<sup>-3</sup>.

The radial distribution functions ( $g_{OO}(r)$ ,  $g_{HH}(r)$ ,  $g_{OH}(r)$ ) and the velocity autocorrelation functions ( $C_O(t)$ ,  $C_H(t)$ ) were calculated from the configurations generated during the simulations. The structure factors ( $S_{OO}(k)$ ,  $S_{HH}(k)$ ,  $S_{OH}(k)$ ) and the spectral densities ( $\hat{S}_H(\omega)$ ,  $\hat{S}_O(\omega)$ ) were calculated as the Fourier transform of the corresponding  $g(r)$  and  $C(t)$  functions. The HBs among neighbouring water molecules were identified during the simulations according to the definition in section 4.

## 3. Structure

In order to compare our MD results with those from the neutron scattering measurements for D<sub>2</sub>O [1] we computed the intermolecular composite  $g(r)$  function defined as a combination of the partial  $g(r)$ s for H<sub>2</sub>O and the weighting factors corresponding to D<sub>2</sub>O [7] (it should be remembered that the structure from classical MD simulations is independent of the mass)

$$g(r) = 0.092g_{OO}(r) + 0.422g_{OH}(r) + 0.486g_{HH}(r). \quad (1)$$

The intramolecular contributions to  $g_{OH}(r)$  and  $g_{HH}(r)$  were removed. The structure factor ( $S(k)$ ) corresponding to the composite  $g(r)$  function shows a symmetric peak and weak overdamped oscillations (figure 1) which reflect a loss of the orientational correlations. These findings are in good agreement with both experimental data and MD results using the NEMO potential [1].

The resulting  $S_{OO}(k)$  does not show the double-structured first peak observed at room temperature and the oscillations after the first maximum are rather smooth (figure 1). These

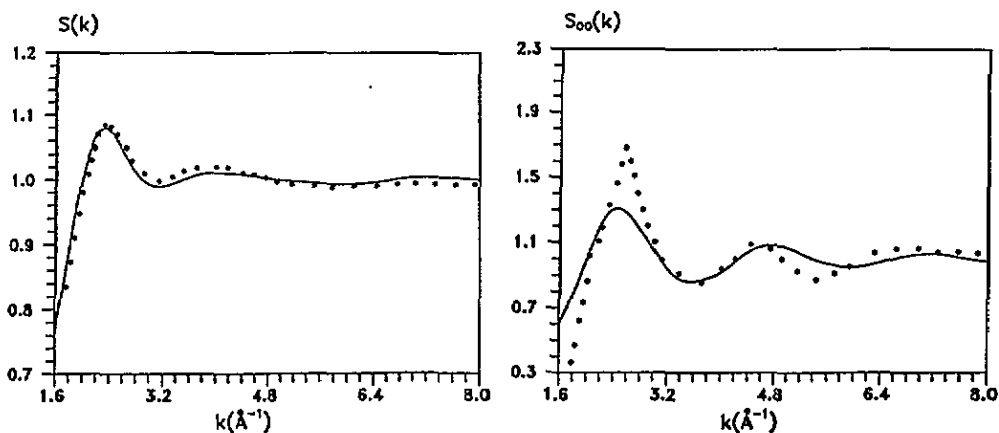


Figure 1. The  $S(k)$  and  $S_{OO}(k)$  structure factors obtained from the MD simulation at 523 K (—), compared with experimental results (\*\*\*\*) at the same temperature [1].

findings are in qualitative agreement with those from neutron diffraction and indicate that the tetrahedral ordering associated with the directionality of the HBS is greatly reduced at high temperature [1]. However, marked quantitative differences between our  $S_{OO}(k)$  and the experimental results may be observed. These can be attributed to shortcomings of the potential model. Nevertheless, it should be remembered that measurements of partial structure factors are difficult and ordinarily have large errors. In the case of water at room temperature the discrepancies between the height of the first maximum of the  $g_{OO}(r)$  function obtained from x-rays and neutron scattering is about 25% [2] (this discrepancy is of the same order of magnitude as in figure 1). Moreover, the experimental  $S_{OO}(k)$  function is a preliminary result for a mixture of  $H_2O$  and  $D_2O$  (null water). MD results for  $S_{OO}(k)$  using the NEMO potential have not been reported [1].

The agreement between our  $S(k)$  and the experimental data at 523 K suggests that the H-H and O-H distributions are well reproduced by our simulations (according to equation (1) the contribution of  $g_{OO}(r)$  to  $g(r)$  is small). MD results at room temperature also show that the  $g_{HH}(r)$  and  $g_{OH}(r)$  functions obtained with the SPC model are close to the experimental data whereas the  $g_{OO}(r)$  function predicted by SPC is too little structured [2]. According to recent MD simulations from 238 to 368 K employing a flexible 'ab initio' potential [8] the results represented in figure 2 show that the peaks of the partial  $g(r)$ s become lower and slightly shifted towards greater distances when  $T$  increases. This reflects less of a correlation in the relative orientation of neighbouring molecules at high temperatures.

The sharp first maximum and deep first minimum  $g_{OH}(r)$  at room temperature is attributed to the formation of strong HBS. Thus, the smooth shape of  $g_{OH}(r)$  at 523 K reflects the weakness of the HB network at this temperature. The results for  $g_{OO}(r)$  imply that the first hydration shell becomes expanded and the separation between the first and second shell is less defined when  $T$  increases. As a consequence of this the O-O-O angles are less defined and the tetrahedral structure of the HB network should be substantially destroyed at 523 K. These results are consistent with the experimental findings by scattering techniques between 262 and 313 K [7]. Although the number of molecules in each shell cannot be determined exactly we have verified that the coordination functions  $n(r)$  (defined as the mean number of atoms within a sphere of a given radius  $r$ ) at the two temperatures do not show marked differences.

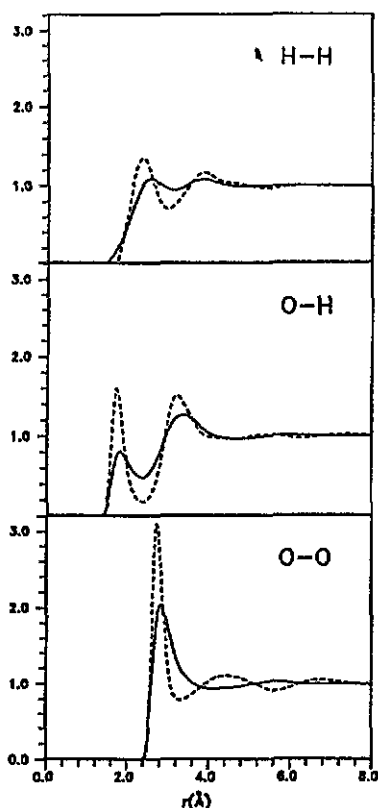


Figure 2. Partial radial distribution functions resulting from the MD simulations at 523 K (—) and 298 K (---).

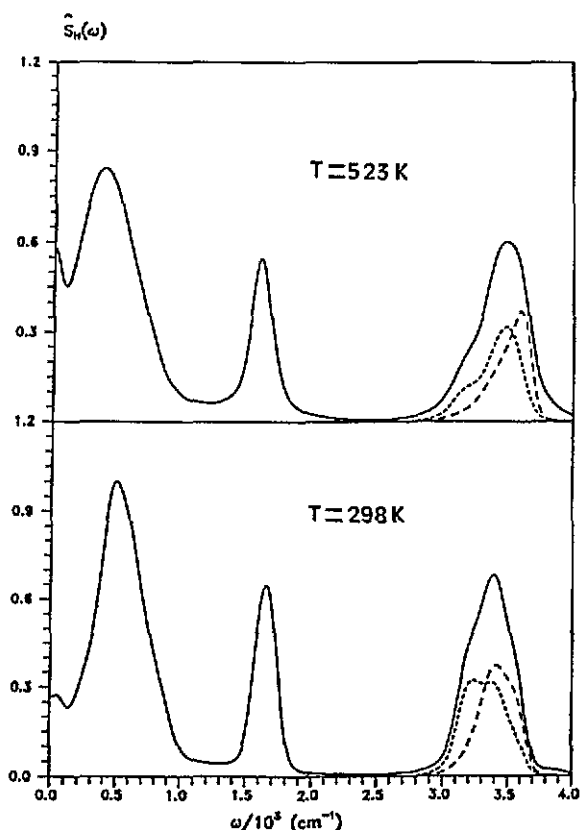


Figure 3.  $\hat{S}_H(\omega)$  spectral densities at 523 K (top) and 298 K (bottom). The full curves were calculated from the  $C_H(r)$  functions. The symmetric (---) and asymmetric (—) contributions to the stretching were determined according to the procedure described in [18, 19].

#### 4. Hydrogen bonds

The structural results presented in the last section indicate that the HB network of water is significantly destroyed when  $T$  increases. In order to perform a quantitative study of the changes in the number and characteristics of the HBs we determined the HBs existing in the MD configurations at 298 and 523 K. Unfortunately the H-bonded molecules cannot be unambiguously distinguished since the intermolecular energy is described by a continuous potential and the adoption of a criterion for deciding when two neighbouring molecules are H bonded is somewhat arbitrary. Different HB definitions which are based on energetic or geometrical criteria have been proposed [9].

We adopted a geometrical definition similar to that recently used by Luzar and Chandler [10]. We assumed that a pair of water molecules are H bonded when two conditions are fulfilled, i.e. the distance between the O atoms is smaller than  $R_{OO}$  and the distance between the O atom of one molecule and the H atom of the other is smaller than  $R_{OH}$ . As cut-off distances we chose the positions of the first minima of the  $g_{OO}(r)$  and  $g_{OH}(r)$  functions at 298 K, i.e.  $R_{OO} = 3.5 \text{ \AA}$  and  $R_{OH} = 2.1 \text{ \AA}$ . One of the advantages of this HB definition is that we can identify the H atom that is directly H bonded to the O of the other molecule.

We employed this definition for the HBs between molecules to classify the atoms in each MD configuration. We considered two classes for the H atoms: the H atoms which participate in a HB and those which do not participate in any HB. In the case of the O atoms we considered three classes: the O atoms which are directly H bonded to two or more H atoms of different molecules, the O atoms which are directly H bonded to only one H atom of another molecule and the O atoms which are not directly H bonded to any molecule.

The averaged percentages of atoms of the classes defined in the last paragraph are presented in table 1. The percentages corresponding to the H atoms at the two temperatures are approximately reversed. Thus the number HBs destroyed when  $T$  increases from 298 to 523 K is 40% of the number of HBs existing at 298 K. The percentages of O atoms with one direct HB is similar for the two temperatures but marked differences are found for the other two classes. The number of O atoms with two or more direct HBs is dramatically reduced when  $T$  increases from 298 to 523 K (the reduction is about 70% of the number of O atoms of this class at 298 K). This is consistent with a significant decrease of the tetrahedral ordering predicted by the structural results. Therefore, although the number of HBs at 523 K is still important, the tridimensional network associated with the O atoms with two or more HBs should be significantly destroyed and probably reduced to one-dimensional chains. We estimated the lifetimes of the HBs using a procedure described elsewhere [9] (intermittent lifetime). As expected, the lifetimes are of the order of 1 ps and they decrease when  $T$  increases. The relation between the mean lifetime at 298 and 523 K is about a factor of two.

Table 1. Percentages of H-bonded atoms.

	$T = 298 \text{ K}$	$T = 523 \text{ K}$
H-bonded hydrogens (%)	60	36
Non-H-bonded hydrogens (%)	40	64
Oxygens without direct HBs (%)	18	39
Oxygens with one direct HB (%)	47	50
Oxygens with two or more direct HBs (%)	35	11

## 5. Dynamic properties

We calculated the self-diffusion coefficients  $D$  as time integrals of the  $C_O(t)$  functions (the motions of the centres of mass of the molecules are very close to those of the O atoms). We also determined  $D$  as the slope of the mean square displacements of the oxygens. The results using the two methods do not show significant differences. The values obtained from the MD simulations are compared with the experimental findings [11, 12] in table 2. As may be observed, the agreement is good at both temperatures. It should be noted that

Table 2. Self-diffusion coefficients (in  $\text{cm}^2 \text{s}^{-1}$ ).

	$T = 298 \text{ K}$	$T = 523 \text{ K}$
MD simulation	$2.5 \times 10^{-5}$	$2.6 \times 10^{-4}$
Experimental	$2.3 \times 10^{-5}$ [11]	$2.8 \times 10^{-4}$ [12]

the  $D$ -value resulting from MD simulations at room temperature with the NEMO potential ( $1.3 \times 10^{-5} \text{ cm}^2 \text{ s}^{-1}$ ) [2] is markedly smaller than the experimental value.

The resulting spectral densities for H ( $\hat{S}_H(\omega)$ ) at the two studied temperatures are shown in figure 3 and table 3. The larger  $\hat{S}_H(0)$  value at 523 K is consistent with the greater weight of the translational modes and the larger  $D$  coefficient at higher temperatures. The maxima of  $\hat{S}_H(\omega)$  may be associated with the peaks of the infrared (IR) spectra. The three bands of  $\hat{S}_H(\omega)$  correspond to the librational ( $200\text{--}1000 \text{ cm}^{-1}$ ), bending ( $1300\text{--}2000 \text{ cm}^{-1}$ ) and stretching ( $2800\text{--}4000 \text{ cm}^{-1}$ ) modes [13]. The marked differences between the librational frequencies at the two temperatures are consistent with the important changes in the intermolecular correlations revealed by the structural results. The frequencies of the peaks for bending and stretching at 298 K are in good agreement with the IR experimental data [14]. Experimental information about the IR spectra at 523 K is rather scarce. MD findings show that the peaks become closer to the frequencies corresponding to the gas phase when  $T$  increases (see table 3). IR measurements by Josien [15] also indicate that the bending frequency is lowered when  $T$  increases. However, other IR [16] and Raman [17] experiments did not find significant shifts for the bending band. The slight increase of the stretching frequency with  $T$  obtained by MD is consistent with the experimental findings [16, 17]. This shift is attributed to the greater number of non-H-bonded molecules at higher temperatures [13].

Table 3. Peaks of the spectral densities and IR spectra (in  $\text{cm}^{-1}$ ). Values in parentheses are the peaks in the experimental IR spectra for liquid water at 298 K [14] and 523 K [15].

	$T = 298 \text{ K}$	$T = 523 \text{ K}$	Gas phase <sup>a</sup>
Libration	500	370	—
Bending	1650 (1645)	1590	1520
Stretching	3385 (3390)	3480	—
Symmetric stretching	3370	3475 ( $\approx 3495$ )	3685
Asymmetric stretching	3410	3595 ( $\approx 3605$ )	3785

<sup>a</sup> Obtained from MD simulations of isolated water molecules [5].

The intramolecular stretching motions of water molecules are ordinarily analysed as a combination of the symmetric and asymmetric vibrations. So, the stretching bands may be considered as a superposition of two frequency bands. These bands can be separately determined during the MD simulations. The method for the calculation is based on the combination of the velocities of the H atoms of each molecule so that the symmetric and asymmetric stretching motions are approximately described [18, 19]. The results obtained by this method at 523 K are in quite good agreement with the IR experiments [15] (table 3). However, the results at 298 K cannot be checked because the peaks corresponding to the symmetric and asymmetric modes cannot be distinguished from IR measurements at this temperature.

Experimental information on the intermolecular vibrations is provided by the far-IR spectra. The maxima of the  $\hat{S}_O(\omega)$  functions obtained by MD may also be associated with the

intermolecular motions and compared with the far-IR spectra. The resulting  $\hat{S}_O(\omega)$  functions (figure 4) show that the pure translational modes ( $\omega = 0$ ) are predominant at 523 K whereas a peak close to  $50 \text{ cm}^{-1}$  and a shoulder around  $200 \text{ cm}^{-1}$  may be observed at 298 K. These bands were also found in far-IR measurements at room temperature [13, 20]. We do not have available data for the far-IR spectra at 523 K but it was observed that both the peak and the shoulder become less pronounced when  $T$  increases [13, 20]. This is in accord with the results in this work. The far-IR spectra of water at room temperature has been related to the existence of HBs and the  $50 \text{ cm}^{-1}$  and  $200 \text{ cm}^{-1}$  bands have been attributed to the bending and stretching modes of the O-H...O units [13]. This interpretation is consistent with the extinction of the peak and the shoulder when the HB network has been significantly destroyed.

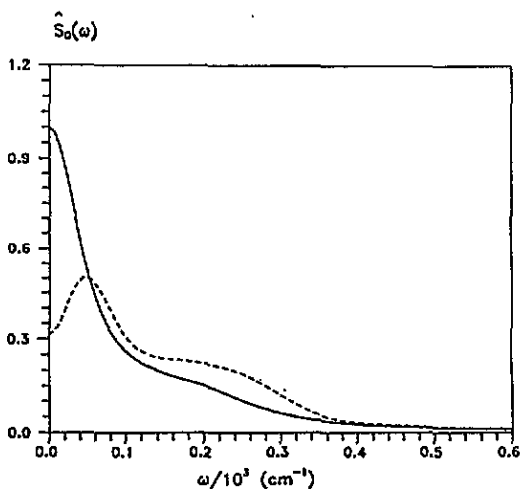


Figure 4.  $\hat{S}_O(\omega)$  spectral densities at 523 K (—) and 298 K (---).

## 6. Concluding remarks

The results of this work corroborate that, despite the simplicity of the SPC potential, MD simulations using this model provide a realistic picture of the microscopic behaviour of liquid water. It was shown [2] that the SPC potential reproduces reasonably the structure and self-diffusion coefficient of water at room temperature. We have verified that these properties are also in good agreement with the experimental data at high temperatures. Moreover, the frequency peaks of the IR and far-IR spectra are also in satisfactory accord with the results of classical MD simulations using a SPC model which incorporates intramolecular degrees of freedom (it should be noted that accurate calculations of the IR spectra would require quantum calculations).

It has been confirmed that properties of liquid water at 523 K approach those of a non-associated liquid. When  $T$  increases from 298 to 523 K there is an important decrease of the number of HBs (40%) and the number of O atoms with two or more direct HBs is dramatically reduced (70%). This implies a significant destruction of the tridimensional HB network which is characteristic of water at room and lower temperatures. These changes are reflected in both the structural and dynamic properties. It has been corroborated that not only the number but also the lifetimes of the HBs are greatly reduced when  $T$  increases.



## Acknowledgments

We would like to thank the 'Centre de Supercomputació de Catalunya' (CESCA) for their computational facilities. The financial support of DGICYT, project PB90-0613-CO3, is also acknowledged.

## References

- [1] Buontempo U, Postorino P, Ricci M A and Soper A K 1992 *Europhys. Lett.* **19** 385
- [2] Walqvist A, Ahlström P and Karlström G 1990 *J. Phys. Chem.* **94** 1649
- [3] Berendsen H J C, Postma J P M, van Gunsteren W F and Hermans J 1981 *Intermolecular Forces* ed B Pullman (Dordrecht: Reidel) pp 331–42
- [4] Anderson J, Ullo J J and Yip S 1987 *J. Chem. Phys.* **87** 1726
- [5] Martí J, Padró J A and Guàrdia E 1994 unpublished
- [6] Toukan K and Rahman A 1985 *Phys. Rev. B* **31** 2643
- [7] Chen S H and Teixeira J 1986 *Adv. Chem. Phys.* **64** 1
- [8] Corongiu G and Clementi E 1992 *J. Chem. Phys.* **97** 2030
- [9] Rapaport D C 1983 *Mol. Phys.* **50** 1151
- [10] Luzar A and Chandler D 1993 *J. Chem. Phys.* **98** 8160
- [11] Krynicki K, Green C D and Sawyer D W 1978 *Faraday Discuss. Chem. Soc.* **66** 199
- [12] Hausser R, Maier G and Noack F 1966 *Z. Naturf. a* **21** 1410
- [13] Walrafen G E 1972 *Water, A Comprehensive Treatise* vol 1, ed F Franks (New York: Plenum) pp 158–201
- [14] Bertie J E, Ahmed M K and Eysel H E 1989 *J. Phys. Chem.* **93** 2210
- [15] Josien M L 1967 *Discuss. Faraday Soc.* **43** 142
- [16] Maréchal Y 1991 *J. Chem. Phys.* **95** 5565
- [17] Ratcliffe C I and Irish D E 1982 *J. Phys. Chem.* **86** 4897
- [18] Bopp P 1986 *Chem. Phys. Lett.* **106** 205
- [19] Martí J, Padró J A and Guàrdia E 1993 *Mol. Simul.* at press
- [20] Hasted J B, Husain S K, Frescura F A M and Birch J R 1985 *Chem. Phys. Lett.* **118** 622